Supplement of Geosci. Model Dev., 18, 8439–8460, 2025 https://doi.org/10.5194/gmd-18-8439-2025-supplement © Author(s) 2025. CC BY 4.0 License.





## Supplement of

Benchmarking and evaluating the NASA Land Information System (version 7.5.2) coupled with the refactored Noah-MP land surface model (version 5.0)

Cenlin He et al.

Correspondence to: Cenlin He (cenlinhe@ucar.edu)

The copyright of individual parts of the supplement might differ from the article licence.

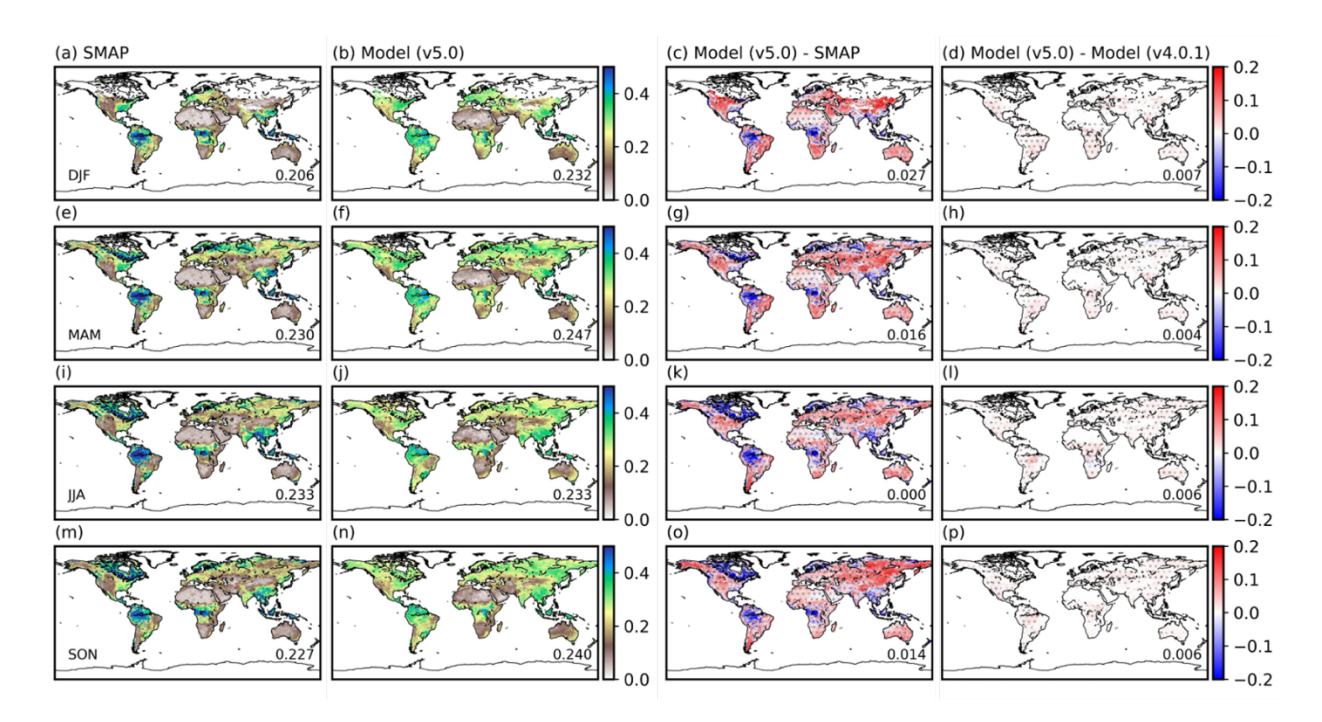


**Figure S1**. Surface soil moisture ( $m^3/m^3$ ) comparison between SMAP observations and LIS/Noah-MP simulations driven by the USAF forcing globally averaged during 2018-2022: (a,e,i,m) SMAP data, (b,f,j,n) LIS/Noah-MPv5.0 simulation, (c,g,k,o) LIS/Noah-MPv5.0 biases (model minus SMAP), and (d,h,l,p) differences between LIS/Noah-MPv5.0 and LIS/Noah-MPv4.0.1 simulations, during four seasons including (a-d) DJF, (e-h) MAM, (i-l) JJA, and (m-p) SON. Grids with statistically significant differences (p < 0.05) are shown with gray dots in the third and fourth columns. The statistical significance over each grid is computed using daily time series and the t-test method. The global mean value is also provided in the lower right of each panel.

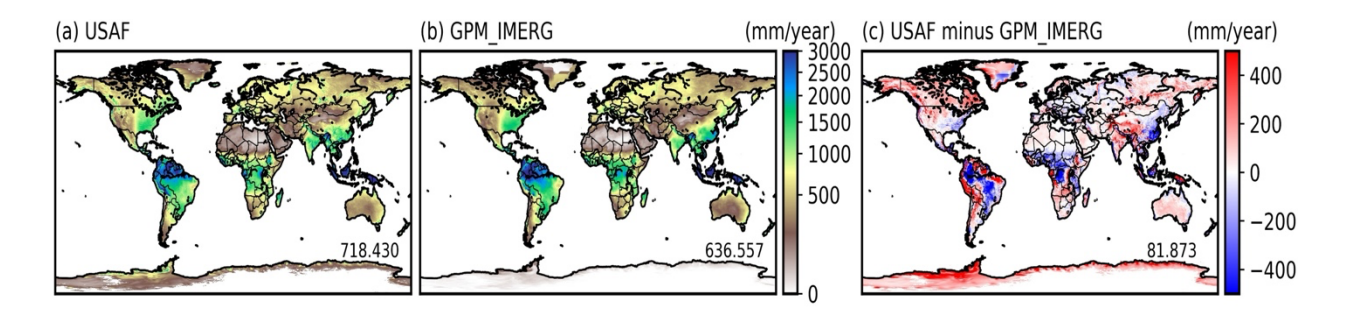


**Figure S2**. Precipitation (mm/year) comparison between the GPM/IMERG data and the USAF forcing data globally averaged during 2018-2022: (a) USAF data, (b) GPM/IMERG data, (c) difference between USAF and GPM/IMERG. The color scale for (a) and (b) is plotted in power law ( $y = x^c$ , where power c = 0.5).

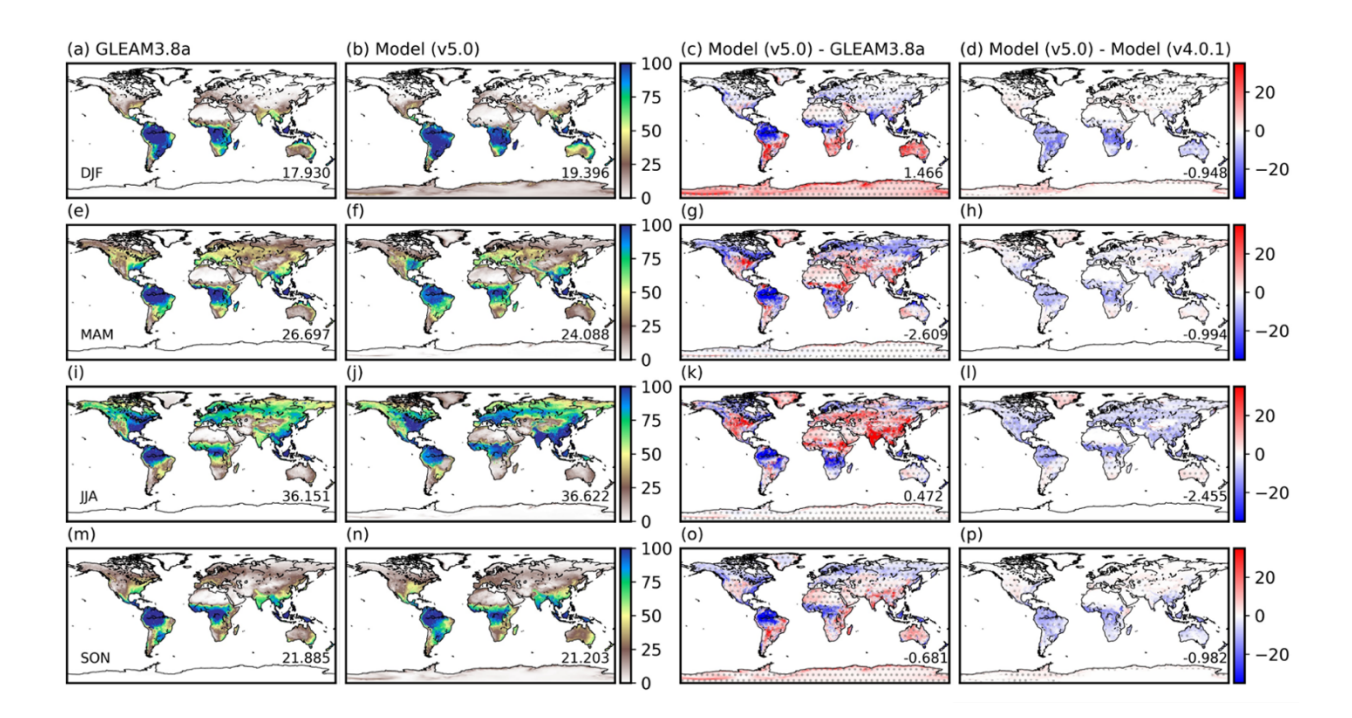


**Figure S3**. Latent heat flux (W/m²) comparison between the GLEAM data and LIS/Noah-MP simulations driven by the USAF forcing globally averaged during 2018-2022: (a,e,i,m) GLEAMv3.8a data, (b,f,j,n) LIS/Noah-MPv5.0 simulation, (c,g,k,o) LIS/Noah-MPv5.0 biases (model minus GLEAM), and (d,h,l,p) differences between LIS/Noah-MPv5.0 and LIS/Noah-MPv4.0.1 simulations, during four seasons including (a-d) DJF, (e-h) MAM, (i-l) JJA, and (m-p) SON. Grids with statistically significant differences (p < 0.05) are shown with gray dots in the third and fourth columns. The statistical significance over each grid is computed using daily time series and the t-test method. The global mean value is also provided in the lower right of each panel.

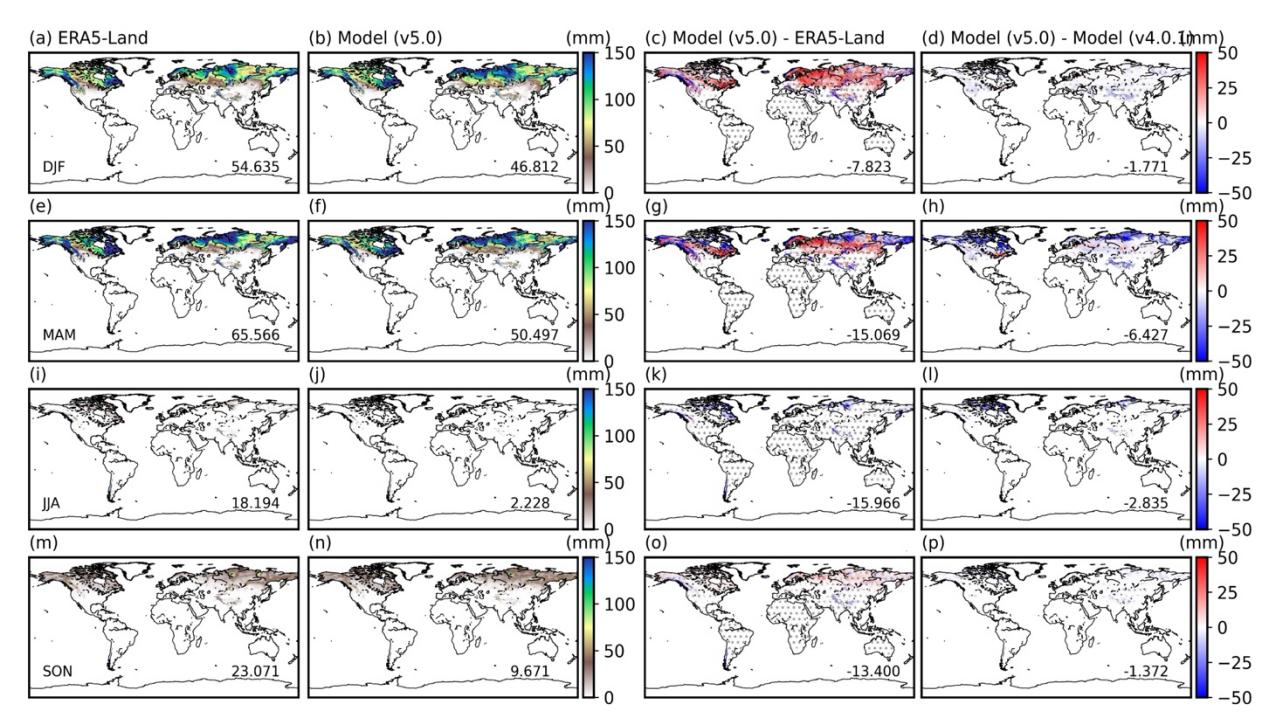


**Figure S4.** SWE (mm) comparison between ERA5-Land and LIS/Noah-MP simulations driven by the USAF forcing globally averaged during 2018-2022: (a,e,i,m) ERA5-Land data, (b,f,j,n) LIS/Noah-MPv5.0 simulation, (c,g,k,o) LIS/Noah-MPv5.0 biases (model minus ERA5-Land), and (d,h,l,p) differences between LIS/Noah-MPv5.0 and LIS/Noah-MPv4.0.1 simulations, during four seasons including (a-d) DJF, (e-h) MAM, (i-l) JJA, and (m-p) SON. Grids with statistically significant differences (p < 0.05) are shown with gray dots in the third and fourth columns. The statistical significance over each grid is computed using daily time series and the t-test method. The global mean value is also provided in the lower right of each panel.

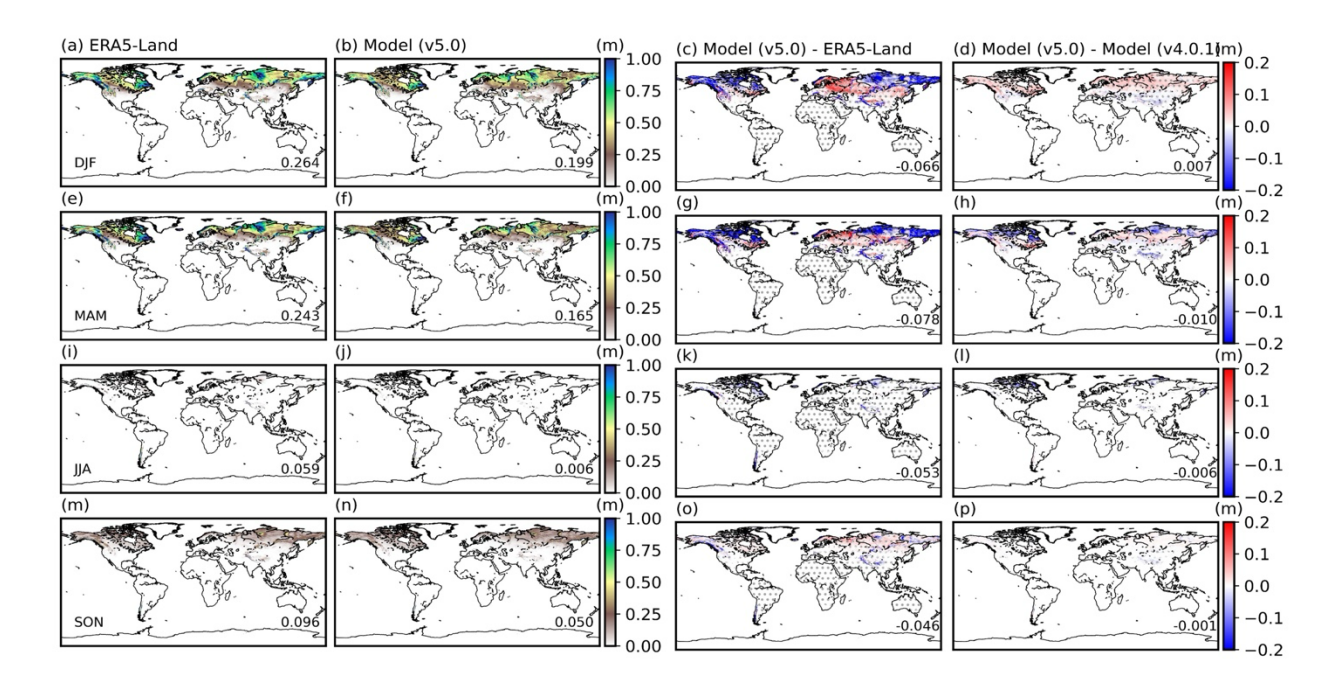


**Figure S5**. Snow depth (m) comparison between ERA5-Land and LIS/Noah-MP simulations driven by the USAF forcing globally averaged during 2018-2022: (a,e,i,m) ERA5-Land data, (b,f,j,n) LIS/Noah-MPv5.0 simulation, (c,g,k,o) LIS/Noah-MPv5.0 biases (model minus ERA5-Land), and (d,h,l,p) differences between LIS/Noah-MPv5.0 and LIS/Noah-MPv4.0.1 simulations, during four seasons including (a-d) DJF, (e-h) MAM, (i-l) JJA, and (m-p) SON. Grids with statistically significant differences (p < 0.05) are shown with gray dots in the third and fourth columns. The statistical significance over each grid is computed using daily time series and the t-test method. The global mean value is also provided in the lower right of each panel.

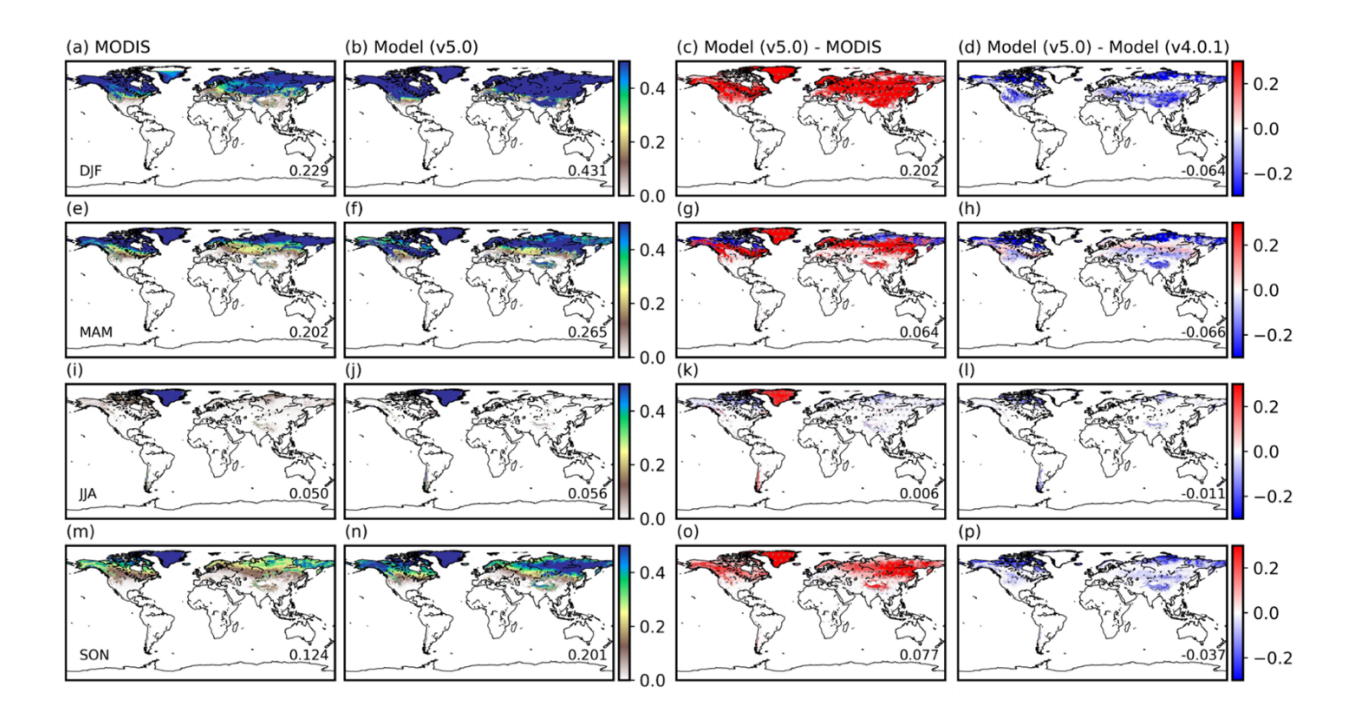


**Figure S6**. Snow cover fraction comparison between MODIS and LIS/Noah-MP simulations driven by the USAF forcing globally averaged during 2018-2022: (a,e,i,m) MODIS data, (b,f,j,n) LIS/Noah-MPv5.0 simulation, (c,g,k,o) LIS/Noah-MPv5.0 biases (model minus MODIS), and (d,h,l,p) differences between LIS/Noah-MPv5.0 and LIS/Noah-MPv4.0.1 simulations, during four seasons including (a-d) DJF, (e-h) MAM, (i-l) JJA, and (m-p) SON. Grids with statistically significant differences (p < 0.05) are shown with gray dots in the third and fourth columns. The statistical significance over each grid is computed using daily time series and the t-test method. The global mean value is also provided in the lower right of each panel.

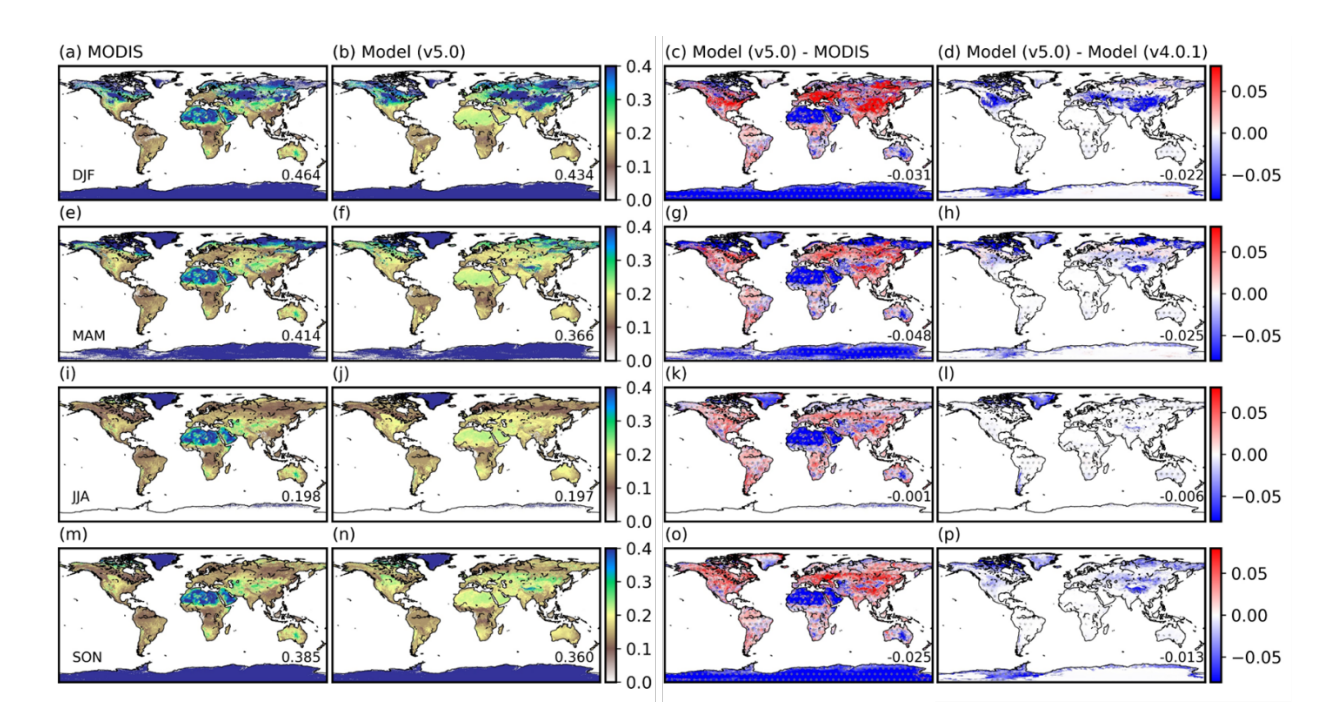


**Figure S7**. Surface albedo comparison between MODIS and LIS/Noah-MP simulations driven by the USAF forcing globally averaged during 2018-2022: (a,e,i,m) MODIS data, (b,f,j,n) LIS/Noah-MPv5.0 simulation, (c,g,k,o) LIS/Noah-MPv5.0 biases (model minus MODIS), and (d,h,l,p) differences between LIS/Noah-MPv5.0 and LIS/Noah-MPv4.0.1 simulations, during four seasons including (a-d) DJF, (e-h) MAM, (i-l) JJA, and (m-p) SON. Grids with statistically significant differences (p < 0.05) are shown with gray dots in the third and fourth columns. The statistical significance over each grid is computed using daily time series and the t-test method. The global mean value is also provided in the lower right of each panel.

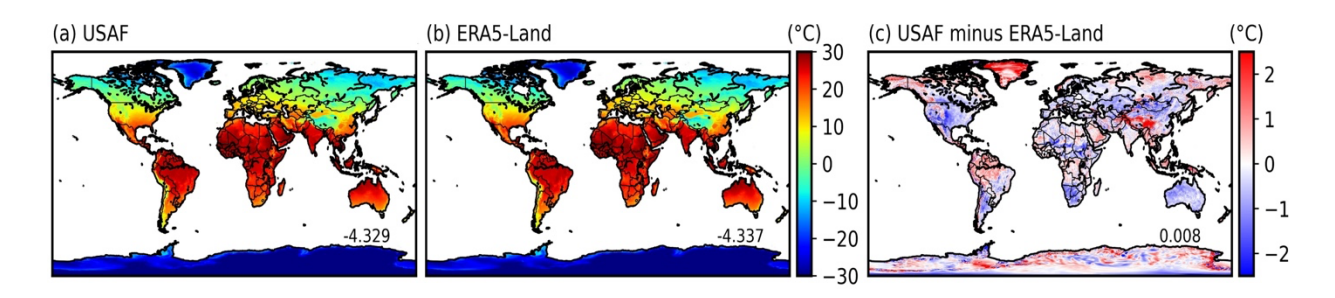


**Figure S8**. Atmospheric temperature forcing (°C) comparison between the ERA5-Land data and the USAF data globally averaged during 2018-2022: (a) USAF data, (b) ERA5-Land data, (c) difference between USAF and ERA5-Land.

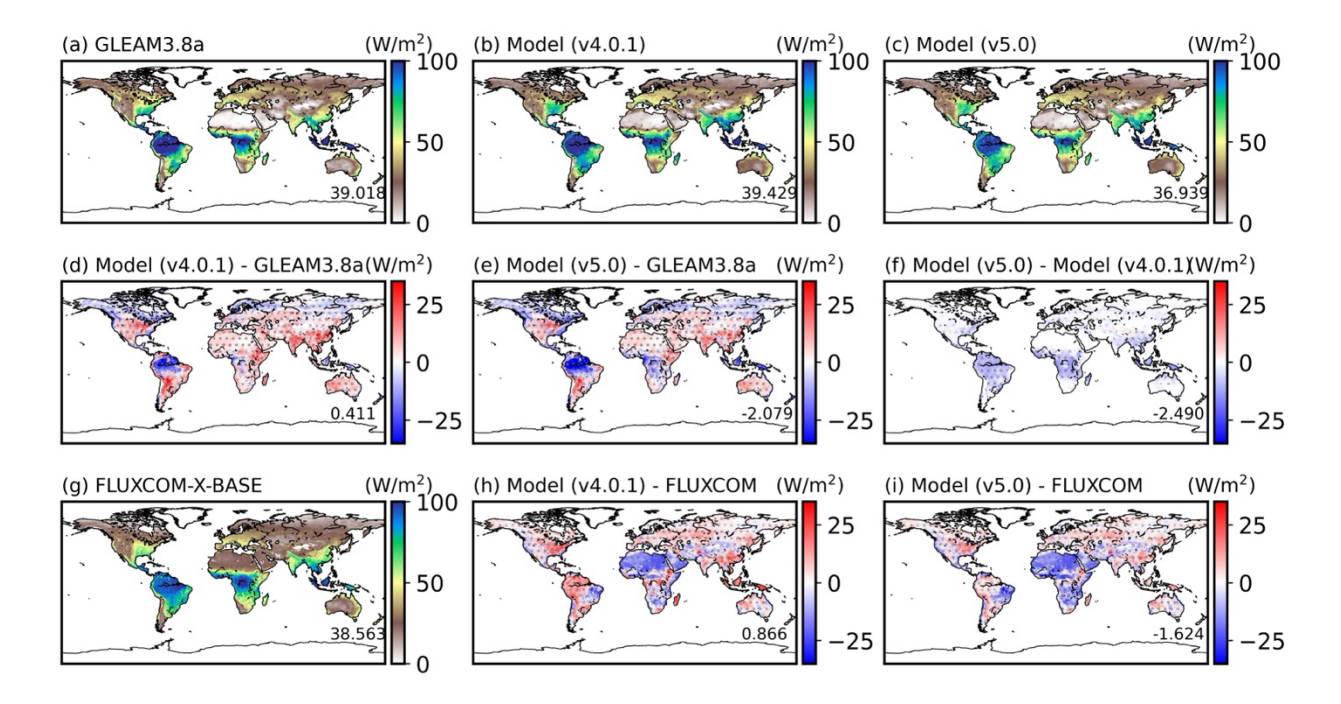


**Figure S9**. Latent heat flux (W/m²) comparison between the GLEAM data, FLUXCOM-X-BASE data, and LIS/Noah-MP simulations driven by the USAF forcing globally averaged during 2018-2021: (a) GLEAM3.8a data, (b) LIS/Noah-MPv4.0.1 simulation, (c) LIS/Noah-MPv5.0 simulation, (d) LIS/Noah-MPv4.0.1 biases (model minus GLEAM), (e) LIS/Noah-MPv5.0 biases (model minus GLEAM), (f) differences between LIS/Noah-MPv5.0 and LIS/Noah-MPv4.0.1 simulations, (g) FLUXCOM-X-BASE data, (h) LIS/Noah-MPv4.0.1 biases (model minus FLUXCOM-X-BASE), and (i) LIS/Noah-MPv5.0 biases (model minus FLUXCOM-X-BASE). Grids with statistically significant differences (p < 0.05) are shown with gray dots in panels (d)-(f). The statistical significance over each grid is computed using daily time series and the t-test method. The global mean value is also provided in the lower right of each panel.

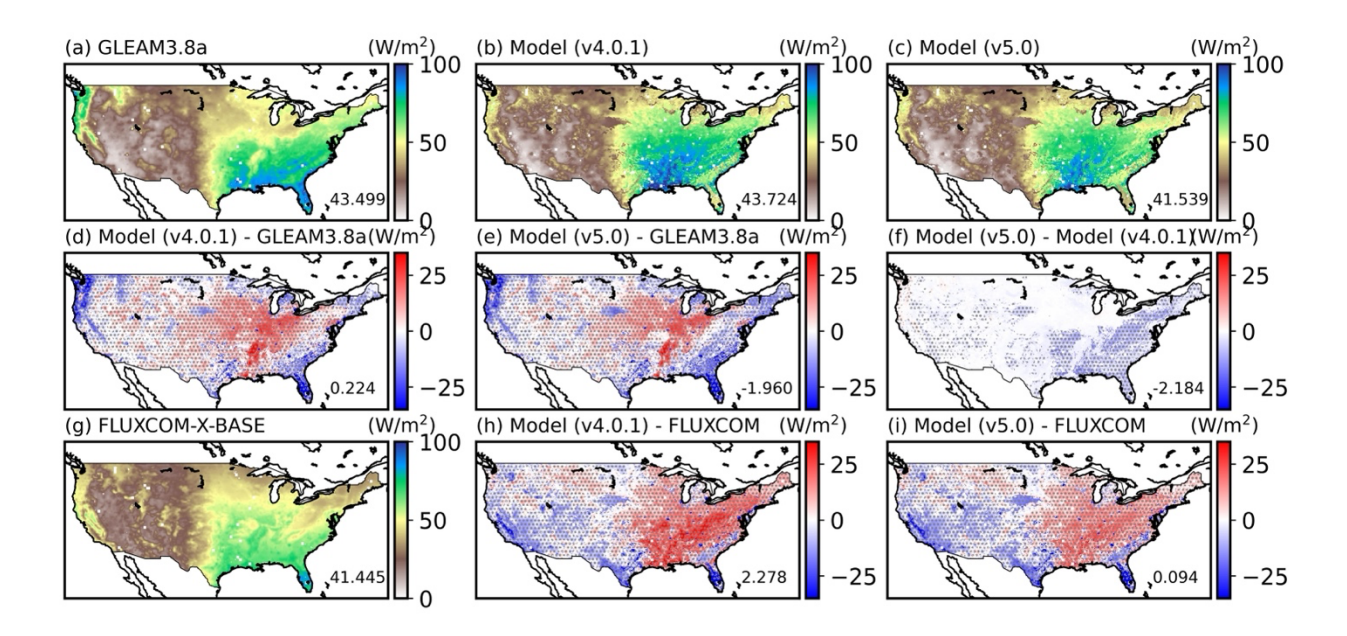


**Figure S10**. Same as Figure S9 but for evaluation of LIS/Noah-MP simulations driven by the NLDAS-2 forcing over the CONUS.

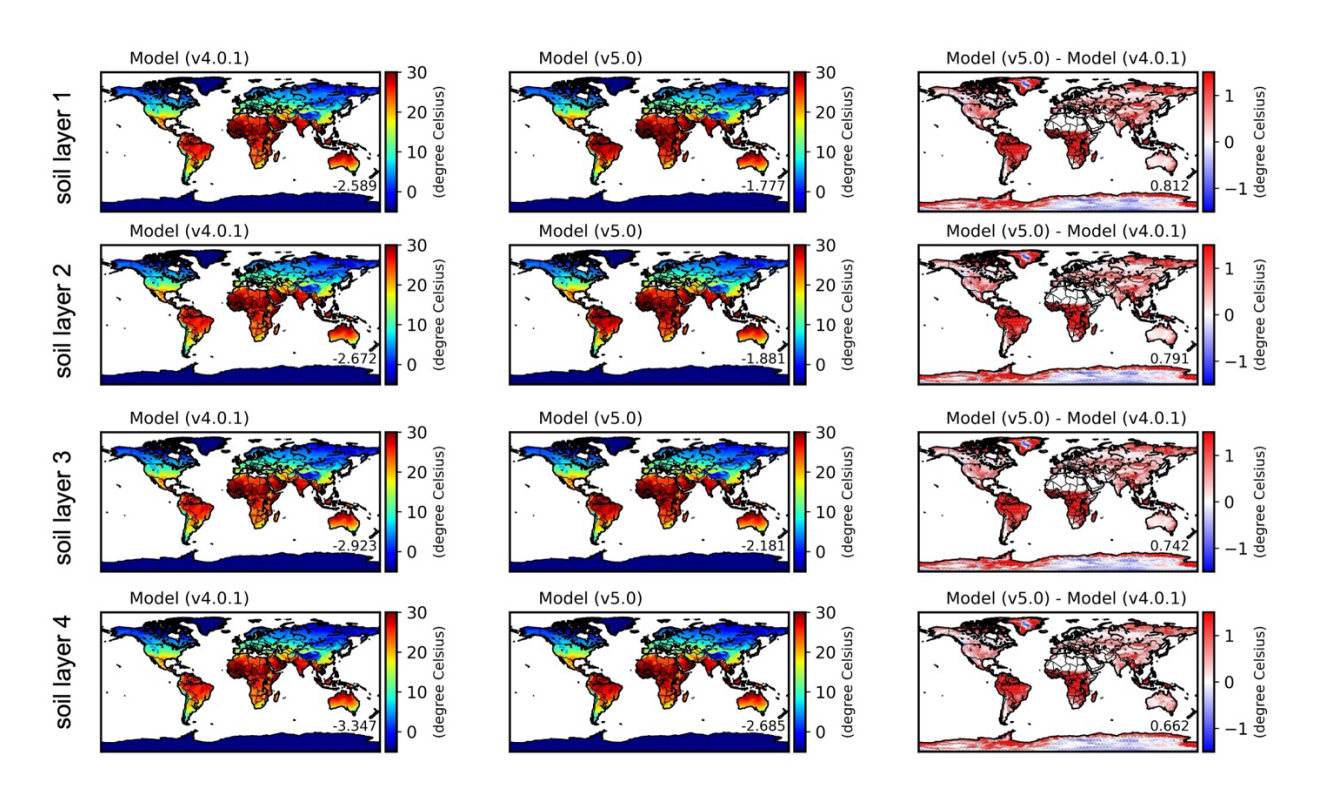


**Figure S11**. Simulated multi-year (2018-2022) annual mean soil temperature from LIS/Noah-MPv4.0.1 (left column), LIS/Noah-MPv5.0 (middle column), and their differences (right column) across four soil layers from the top (layer 1; first row) to the bottom (layer 4; fourth row). The LIS/Noah-MP simulations are driven by the USAF forcing globally. For glacier regions, the temperature is for glacier ice.

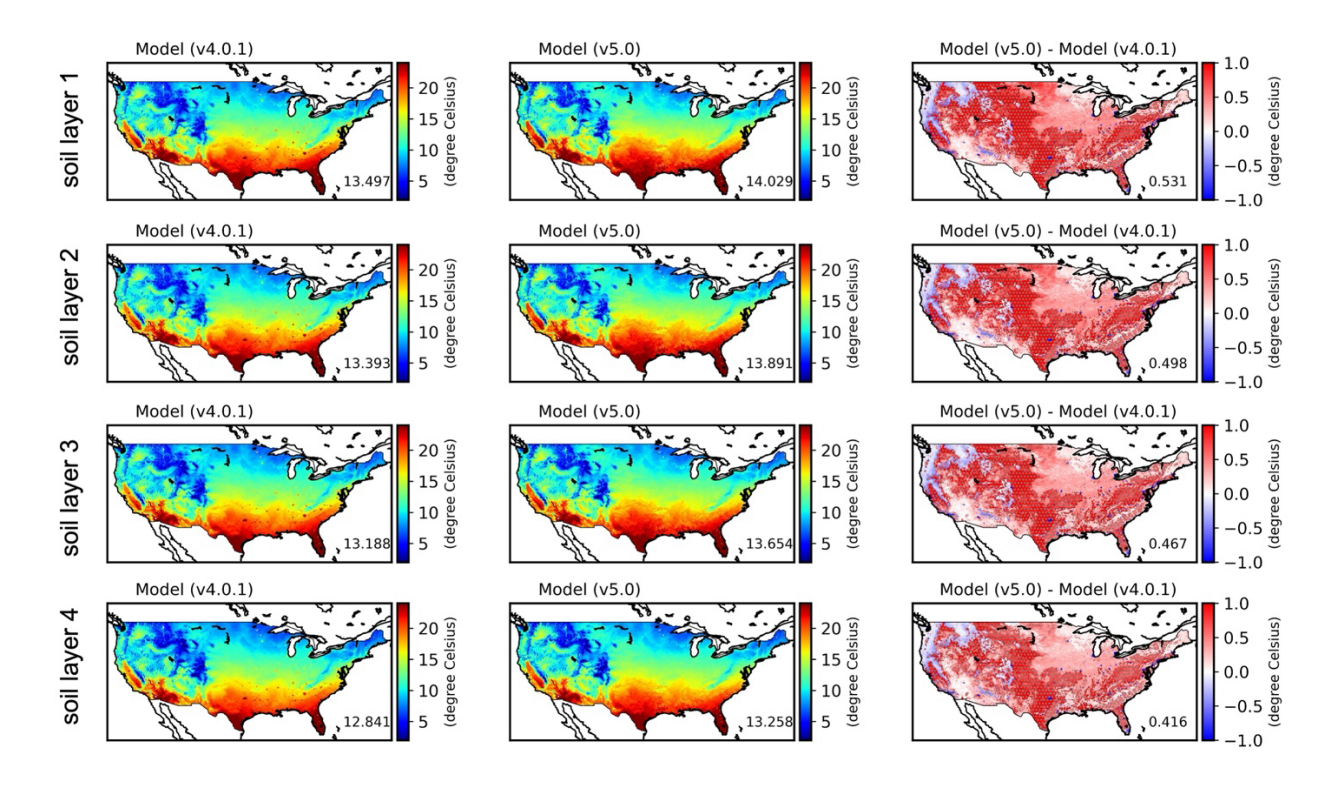


**Figure S12**. Same as Figure S11 but for LIS/Noah-MP simulations driven by the NLDAS-2 forcing over the CONUS.

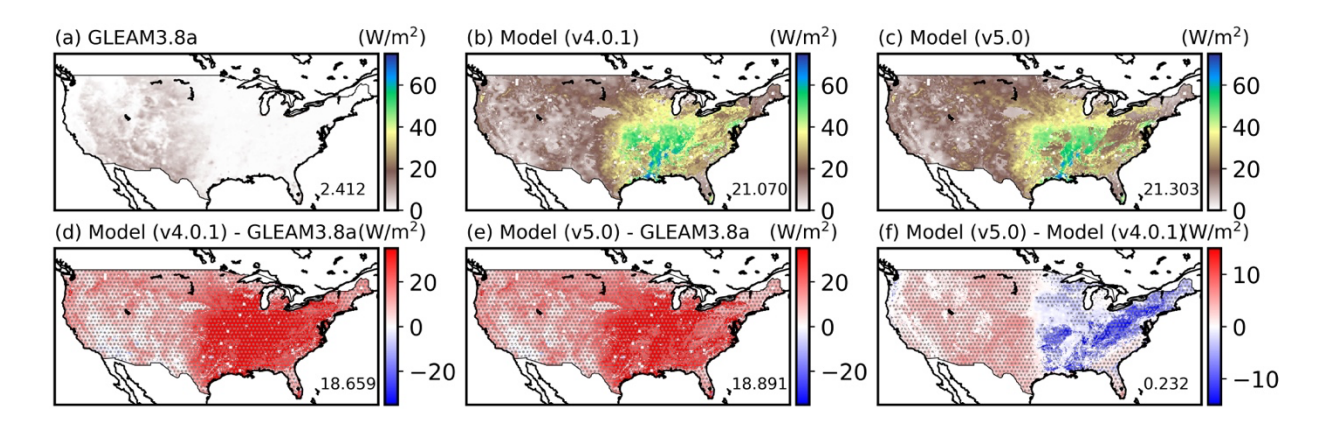


**Figure S13**. Comparison of latent heat flux  $(W/m^2)$  due to soil evaporation between the GLEAM data and LIS/Noah-MP simulations driven by the NLDAS-2 forcing over the CONUS averaged during 2018-2021: (a) GLEAM3.8a data, (b) LIS/Noah-MPv4.0.1 simulation, (c) LIS/Noah-MPv5.0 simulation, (d) LIS/Noah-MPv4.0.1 biases (model minus GLEAM), (e) LIS/Noah-MPv5.0 biases (model minus GLEAM), and (f) differences between LIS/Noah-MPv5.0 and LIS/Noah-MPv4.0.1 simulations. Grids with statistically significant differences (p < 0.05) are shown with gray dots in panels (d)-(f). The statistical significance over each grid is computed using daily time series and the t-test method. The global mean value is also provided in the lower right of each panel. See Figure S16 for seasonal plots.

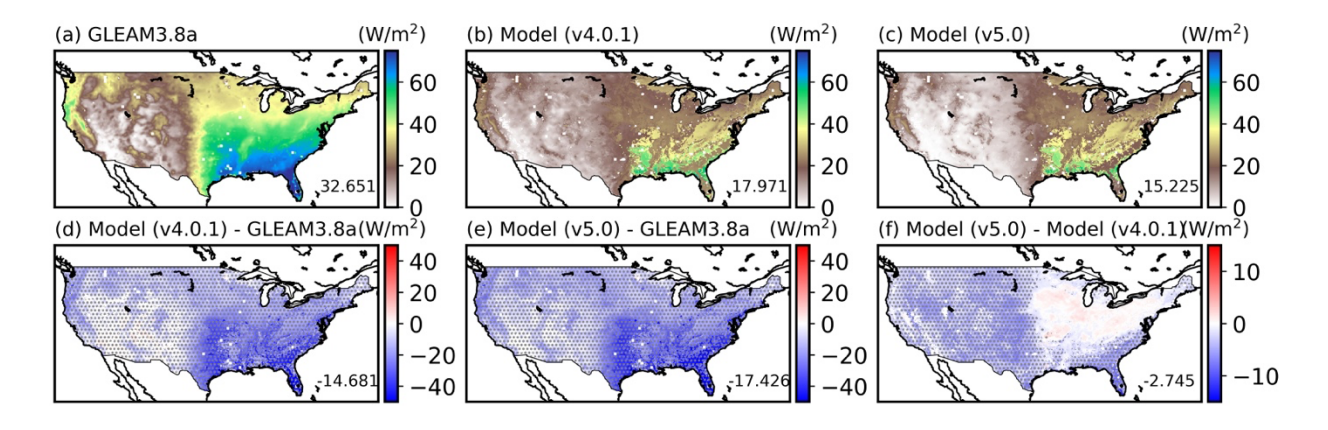


**Figure S14**. Same as Figure S13 but for plant transpiration. See Figure S17 for seasonal plots.

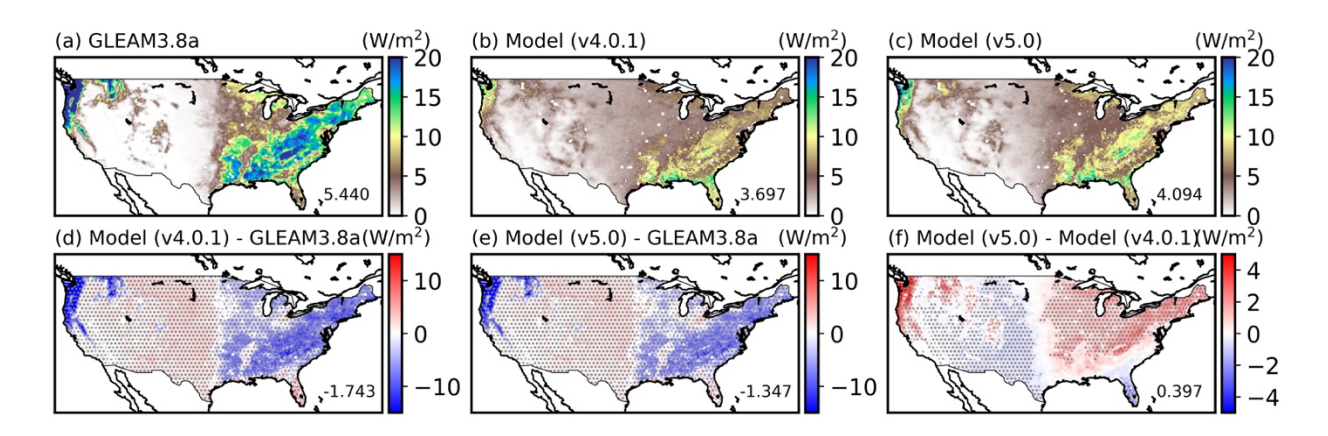


**Figure S15**. Same as Figure S13 but for canopy-intercepted water evaporation. See Figure S18 for seasonal plots.

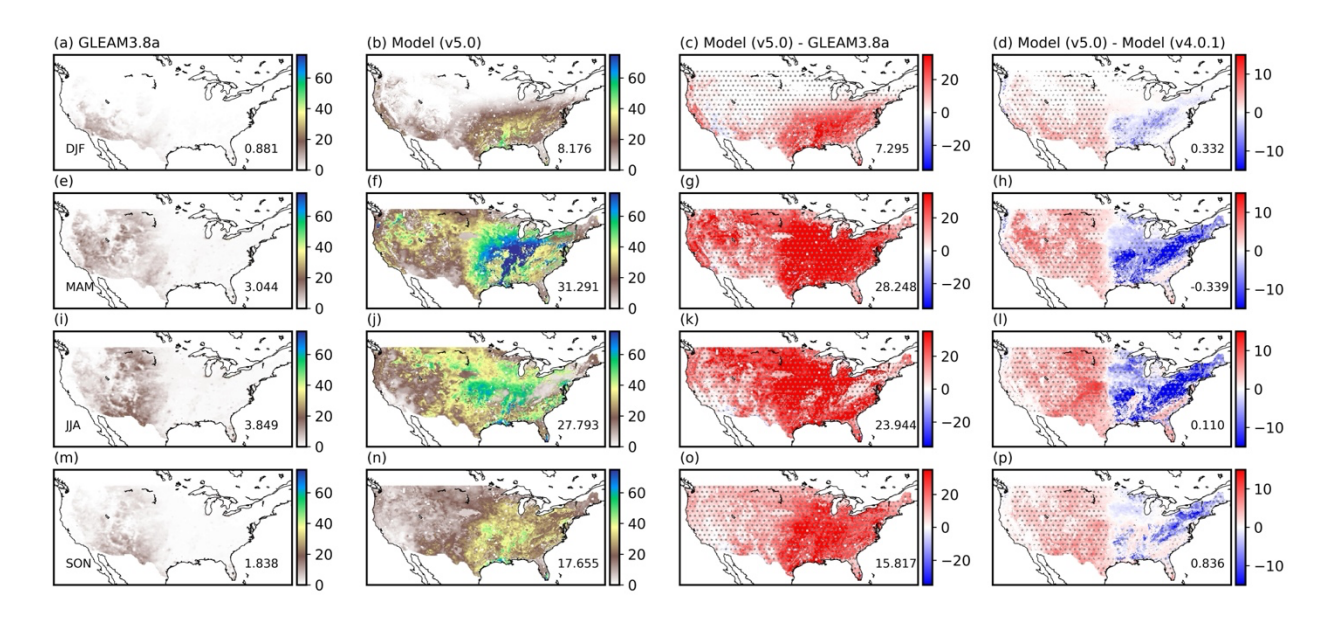


**Figure S16**. Same as Figure S13 but for seasonal results: (a-d) DJF, (e-h) MAM, (i-l) JJA, and (m-p) SON.

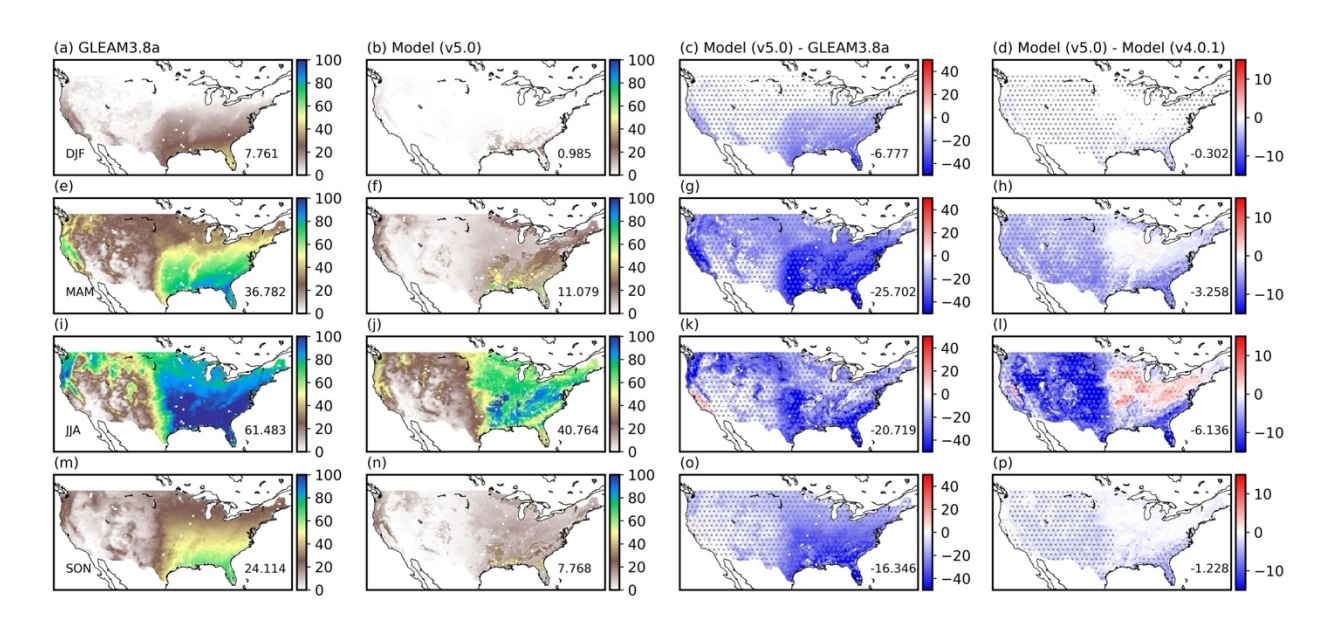


**Figure S17**. Same as Figure S14 but for seasonal results: (a-d) DJF, (e-h) MAM, (i-l) JJA, and (m-p) SON.

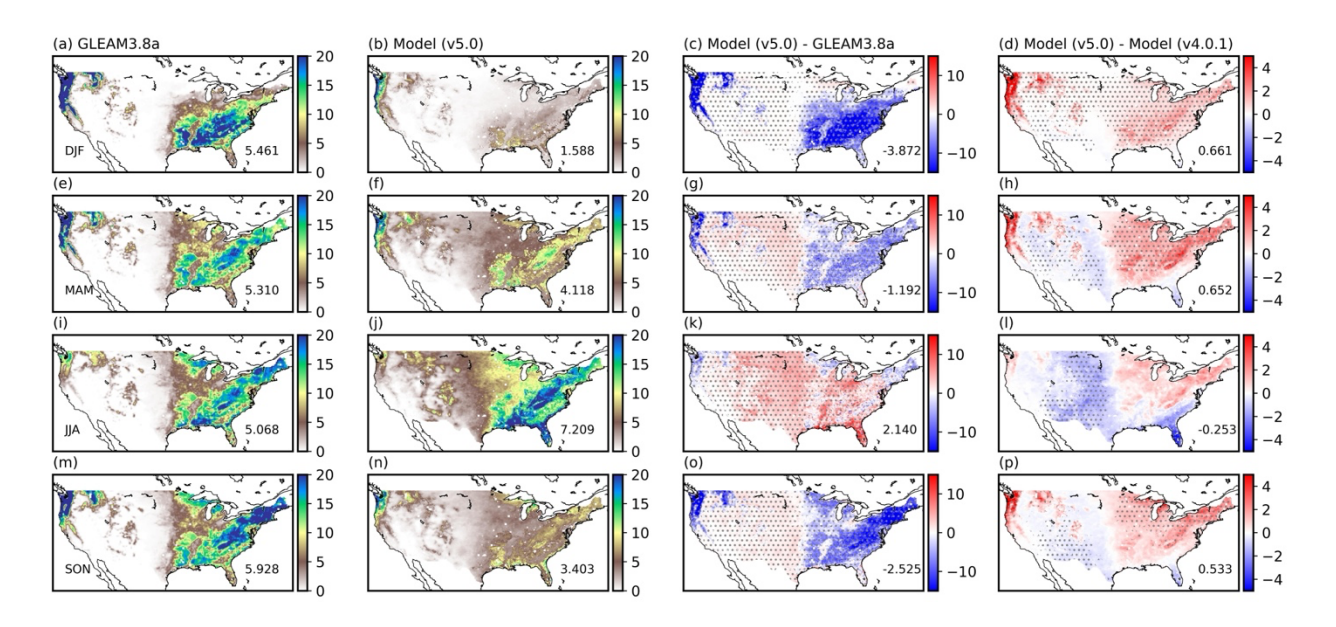


**Figure S18**. Same as Figure S15 but for seasonal results: (a-d) DJF, (e-h) MAM, (i-l) JJA, and (m-p) SON.

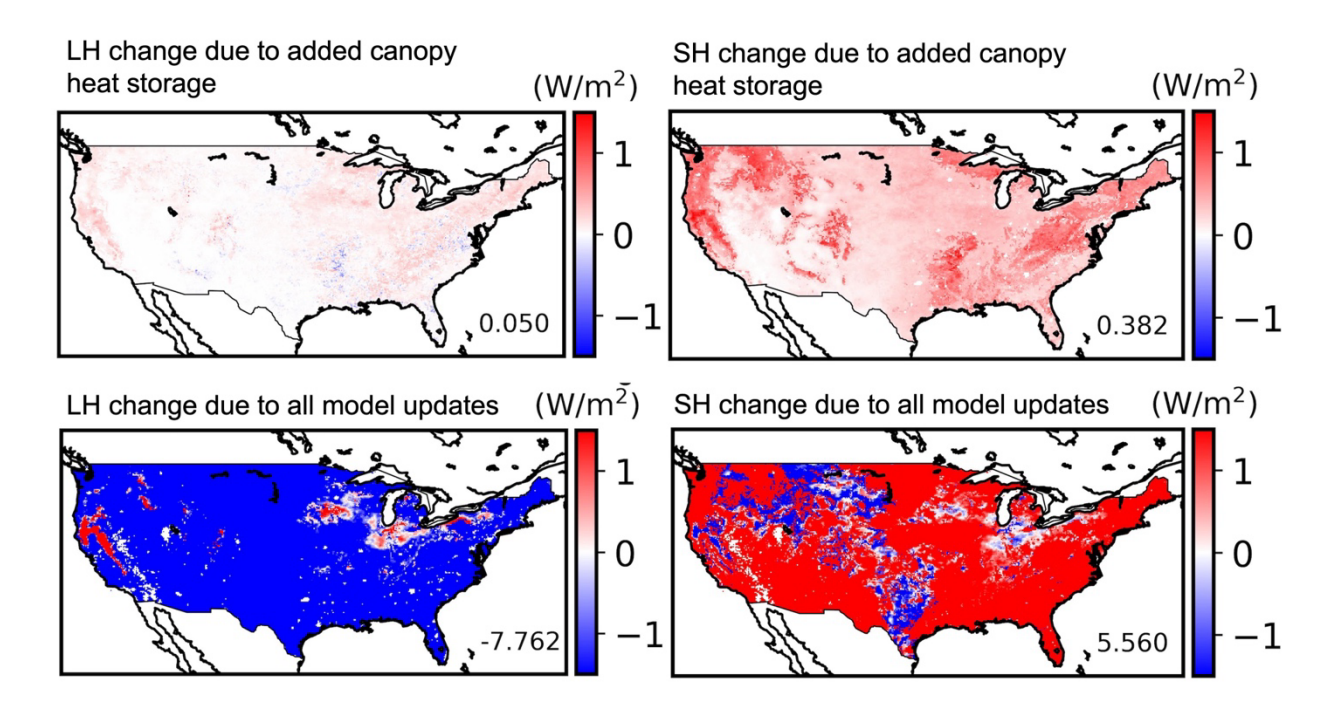


**Figure S19**. Latent heat (LH) and sensible heat (SH) flux changes from LIS/Noah-MPv4.0.1 to LIS/Noah-MPv5.0 due to the added canopy heat storage treatment (first row) and all model updates (second row) in 2018 August.

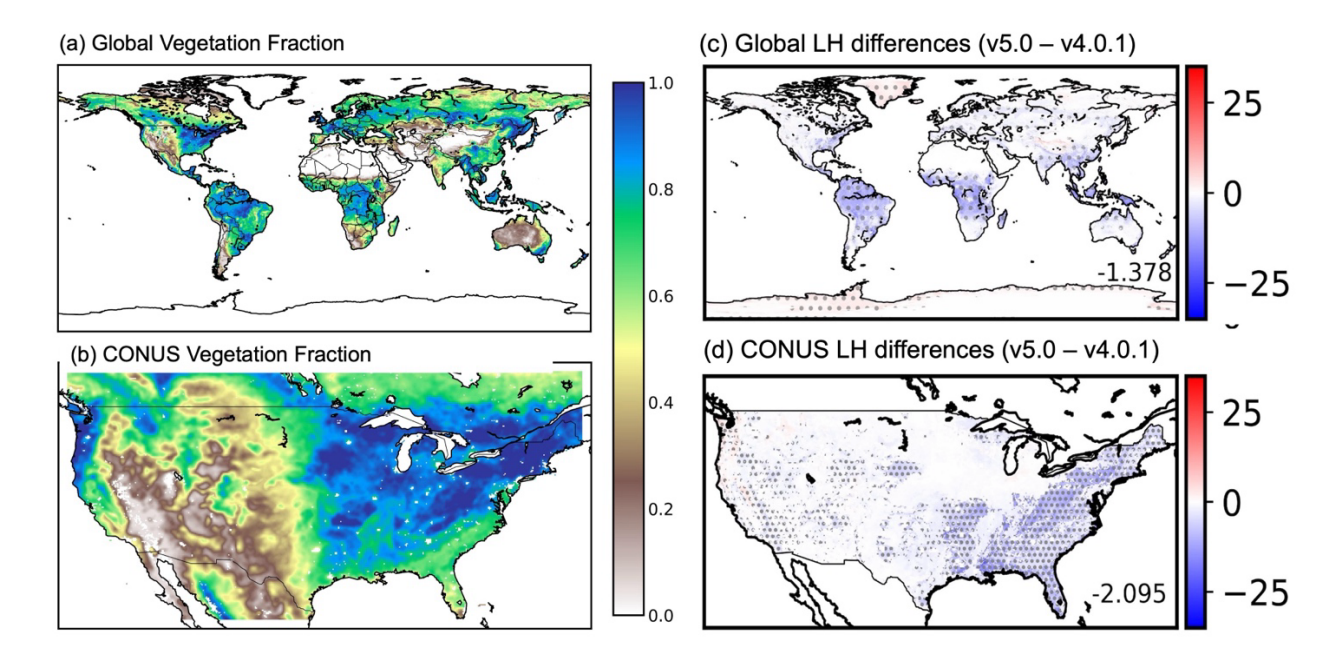


**Figure S20**. Global and CONUS vegetation fraction (a-b) used in the model simulations, and the multi-year (2018-2022) annual mean latent heat (LH) differences (c-d) between LIS/Noah-MPv5.0 and LIS/Noah-MPv4.0.1.

**Table S1.** Model evaluation metrics for LIS/Noah-MPv4.0.1 and LIS/Noah-MPv5.0 simulations driven by the USAF forcing averaged over December-January-February (DJF) during 2018-2022 on the global and regional scale. The values are the mean model bias (LIS/Noah-MP simulations minus reference datasets). The statistically significant difference between LIS/Noah-MP v4.0.1 and LIS/Noah-MPv5.0 simulations (p < 0.05 using a t-test for daily time series) are marked as bold font. The values in the parentheses are the mean absolute model biases.

	Glo	bal	Low la	atitude	Northern midlatitude		Northern high latitude		Southern midlatitude		Southern high latitude	
LIS/Noah-MP	v4.0.1	v5.0	v4.0.1	v5.0	v4.0.1	v5.0	v4.0.1	v5.0	v4.0.1	v5.0	v4.0.1	v5.0
Surface soil moisture (m³/m³ compared to SMAP)	0.020 (0.080)	0.027 (0.083)	-0.004 (0.070)	0.004 (0.072)	0.059 (0.095)	0.066 (0.100)	-0.063 (0.158)	-0.062 (0.157)	0.035 (0.082)	0.043 (0.087)	-	-
Surface Soil moisture (m³/m³ compared to ISMN)	0.052 (0.078)	0.059 (0.084)	0.013 (0.053)	0.022 (0.059)	0.055 (0.081)	0.062 (0.086)	0.096 (0.099)	0.096 (0.099)	0.065 (0.068)	0.068 (0.070)	-	-
Latent heat flux (W/m² compared to GLEAM3.8a)	2.414 (8.184)	1.466 (8.297)	2.141 (16.165)	-3.752 (14.870)	-2.962 (4.229)	-2.449 (4.016)	-0.113 (0.894)	-0.190 (0.916)	12.486 (21.025)	6.452 (18.489)	7.447 (7.659)	9.338 (9.442)
Snow water equivalent (mm compared to ERA5- Land)	-6.051 (26.573)	-7.823 (26.321)	-0.853 (0.984)	-0.883 (1.000)	7.218 (23.983)	5.418 (23.245)	-37.503 (78.639)	-42.473 (79.038)	-8.938 (12.807)	-8.728 (12.370)	-	-
Snow depth (m compared to ERA5-Land)	-0.073 (0.102)	-0.066 (0.100)	-0.003 (0.004)	-0.004 (0.004)	-0.023 (0.083)	-0.015 (0.083)	-0.293 (0.324)	-0.272 (0.315)	-0.031 (0.039)	-0.030 (0.037)	-	-
Snow cover fraction (compared to MODIS)	0.266 (0.267)	0.202 (0.206)	0.004 (0.006)	0.003 (0.004)	0.386 (0.389)	0.311 (0.317)	0.516 (0.516)	0.366 (0.373)	0.005 (0.009)	0.004 (0.009)	-	-
Surface albedo (compared to MODIS)	-0.009 (0.091)	-0.031 (0.093)	-0.018 (0.051)	-0.020 (0.051)	0.094 (0.130)	0.056 (0.102)	0.005 (0.121)	-0.053 (0.172)	0.011 (0.033)	0.009 (0.032)	-0.086 (0.090)	-0.101 (0.103)

Table S2. Same as Table S1 but for March-April-May (MAM) averages.

	Glo	bal	Low l	atitude		thern titude		rn high tude		thern titude	Southern high latitude	
LIS/Noah-MP	v4.0.1	v5.0	v4.0.1	v5.0	v4.0.1	v5.0	v4.0.1	v5.0	v4.0.1	v5.0	v4.0.1	v5.0
Surface soil moisture (m³/m³ compared to SMAP)	0.013 (0.077)	0.016 (0.078)	-0.006 (0.069)	0.000 (0.070)	0.033 (0.082)	0.036 (0.084)	0.009 (0.081))	0.008 (0.081)	0.021 (0.077)	0.030 (0.083)	-	-
Surface Soil moisture (m³/m³ compared to ISMN)	0.048 (0.075)	0.051 (0.077)	0.032 (0.063)	0.040 (0.066)	0.048 (0.075)	0.051 (0.077)	0.106 (0.116)	0.107 (0.117)	0.054 (0.060)	0.057 (0.058)	-	-
Latent heat flux (W/m² compared to GLEAM3.8a)	-1.614 (8.272)	-2.609 (8.499)	-0.028 (13.243)	-4.268 (14.196)	-2.284 (12.144)	-3.301 (12.521)	-6.919 (8.214)	-5.205 (7.419)	-1.425 (6.665)	-0.836 (7.569)	0.448 (1.295)	0.557 (1.306)
Snow water equivalent (mm compared to ERA5- Land)	-8.642 (29.319)	-15.069 (30.461)	-1.064 (1.272)	-1.116 (1.291)	2.464 (26.332)	-1.265 (27.002)	-41.038 (87.507)	-65.033 (92.067)	-9.468 (11.037)	-9.000 (10.882)	-	-
Snow depth (m compared to ERA5-Land)	-0.068 (0.096)	-0.078 (0.107)	-0.004 (0.004)	-0.004 (0.004)	-0.026 (0.075)	-0.027 (0.080)	-0.265 (0.308)	-0.313 (0.354)	-0.032 (0.035)	-0.031 (0.035)	-	-
Snow cover fraction (compared to MODIS)	0.129 (0.131)	0.064 (0.121)	0.001 (0.003)	0.000 (0.002)	0.160 (0.162)	0.126 (0.146)	0.291 (0.291)	0.075 (0.274)	0.005 (0.016)	0.002 (0.014)	-	-
Surface albedo (compared to MODIS)	-0.023 (0.064)	-0.048 (0.081)	-0.020 (0.048)	-0.021 (0.048)	0.029 (0.059)	0.014 (0.056)	-0.054 (0.092)	-0.152 (0.180)	0.018 (0.036)	0.015 (0.035)	-0.063 (0.069)	-0.072 (0.075)

Table S3. Same as Table S1 but for June-July-August (JJA) averages.

	Glo	bal	Low la	atitude		thern atitude	Northern high latitude		Sout midla	thern titude		rn high aude
Noah-MP	v4.0.1	v5.0	v4.0.1	v5.0	v4.0.1	v5.0	v4.0.1	v5.0	v4.0.1	v5.0	v4.0.1	v5.0
Surface soil moisture (m³/m³ compared to SMAP)	-0.005 (0.078)	0.000 (0.079)	-0.016 (0.071)	-0.010 (0.071)	0.012 (0.078)	0.017 (0.081)	-0.023 (0.091)	-0.019 (0.091)	0.022 (0.090)	0.031 (0.096)	-	-
Surface Soil moisture (m³/m³ compared to ISMN)	0.067 (0.085)	0.072 (0.088)	0.024 (0.070)	0.034 (0.075)	0.069 (0.084)	0.074 (0.088)	0.127 (0.131)	0.129 (0.132)	0.039 (0.071)	0.039 (0.070)	-	-
Latent heat flux (W/m² compared to GLEAM3.8a)	2.927 (11.336)	0.472 (10.599)	4.066 (17.233)	-0.412 (16.601)	10.697 (17.801)	5.522 (14.889)	-5.468 (12.165)	-6.020 (12.962)	-4.440 (7.092)	-3.425 (6.825)	0.959 (1.286)	1.012 (1.313)
Snow water equivalent (mm compared to ERA5- Land)	-13.131 (17.021)	-15.966 (17.519)	-0.740 (0.813)	-0.772 (0.821)	-3.316 (8.360)	-5.265 (7.901)	-52.729 (59.916)	-62.524 (63.347)	-10.688 (18.101)	-10.761 (18.218)	-	-
Snow depth (m compared to ERA5-Land)	-0.047 (0.054)	-0.053 (0.056)	-0.003 (0.003)	-0.003 (0.003)	-0.014 (0.024)	-0.018 (0.023)	-0.184 (0.197)	-0.206 (0.208)	-0.043 (0.061)	-0.041 (0.062)	-	-
Snow cover fraction (compared to MODIS)	0.017 (0.030)	0.006 (0.034)	0.000 (0.002)	-0.001 (0.002)	0.001 (0.012)	-0.003 (0.011)	0.060 (0.093)	0.024 (0.112)	0.057 (0.071)	0.039 (0.055)	-	-
Surface albedo (compared to MODIS)	0.005 (0.045)	-0.001 (0.045)	-0.018 (0.049)	-0.019 (0.049)	0.011 (0.037)	0.010 (0.036)	0.027 (0.050)	0.009 (0.051)	0.032 (0.044)	0.023 (0.038)	-0.036 (0.045)	-0.053 (0.059)

Table S4. Same as Table S1 but for September-October-November (SON) averages.

	Global		Low latitude		Northern midlatitude		Northern high latitude		Southern midlatitude		Southern high latitude	
Noah-MP	v4.0.1	v5.0	v4.0.1	v5.0	v4.0.1	v5.0	v4.0.1	v5.0	v4.0.1	v5.0	v4.0.1	v5.0
Surface soil moisture (m³/m³ compared to SMAP)	0.008 (0.080)	0.014 (0.082)	-0.010 (0.065)	-0.004 (0.065)	0.020 (0.080)	0.027 (0.084)	0.014 (0.108)	0.019 (0.110)	0.036 (0.090)	0.042 (0.093)	-	-
Surface Soil moisture (m³/m³ compared to ISMN)	0.066 (0.083)	0.073 (0.088)	0.026 (0.071)	0.034 (0.074)	0.067 (0.083)	0.074 (0.088)	0.120 (0.120)	0.121 (0.121)	0.061 (0.082)	0.061 (0.079)	-	-
Latent heat flux (W/m² compared to GLEAM3.8a)	0.301 (6.785)	-0.681 (7.228)	2.243 (12.533)	-2.624 (13.228)	-2.550 (6.536)	-2.259 (6.910	-3.766 (4.360)	-3.522 (4.166)	-0.550 (10.947)	-3.173 (11.249)	3.204 (3.237)	3.879 (3.883)
Snow water equivalent (mm compared to ERA5- Land)	-12.029 (17.559)	-13.400 (17.511)	-0.698 (0.729)	-0.718 (0.743)	-3.228 (7.672)	-3.980 (7.407)	-47.344 (63.135)	-52.270 (63.555)	-12.553 (22.812)	-12.550 (22.978)	-	-
Snow depth (m compared to ERA5- Land)	-0.045 (0.060)	-0.046 (0.061)	-0.002 (0.003)	-0.003 (0.003)	-0.014 (0.028)	-0.014 (0.028)	-0.175 (0.215)	-0.180 (0.221)	-0.044 (0.065)	-0.043 (0.065)	-	-
Snow cover fraction (compared to MODIS)	0.114 (0.116)	0.077 (0.082)	0.000 (0.001)	-0.001 (0.001)	0.111 (0.116)	0.084 (0.090)	0.297 (0.298)	0.189 (0.195)	0.023 (0.029)	0.020 (0.027)	-	-
Surface albedo (compared to MODIS)	-0.012 (0.065)	-0.025 (0.063)	-0.018 (0.046)	-0.019 (0.046)	0.034 (0.056)	0.025 (0.048)	0.057 (0.066)	0.022 (0.047)	0.013 (0.031)	0.010 (0.029)	-0.088 (0.091)	-0.102 (0.103)